Simultaneous observation of chorus and hiss near the plasmapause

B. Delport,[1] A. B. Collier,[1,2] J. Lichtenberger,[3] C. J. Rodger,[4] M. Parrot,[5] M. A. Clilverd,[6] and R. H. W. Friedel[7]

Received 10 February 2012; revised 13 October 2012; accepted 16 October 2012; published 14 December 2012.

[1] On 4 August 2010 a moderate geomagnetic storm occurred with minimum Dst of −65 nT and maximum K_p of 7−. Shortly after the onset of this storm, VLF chorus was observed at Marion Island (L = 2.6). Over time the spectral structure of the chorus transformed into a hiss band spanning the same frequency range. The observation of overlapping chorus and hiss suggests that Marion Island was close to the plasmapause at the time of this event, and provides ground-based observational confirmation of the generation mechanism of plasmaspheric hiss from chorus waves outside of the plasmasphere. Chorus observations at Marion Island were not common during this period of the solar cycle and so this event was investigated in detail. The geomagnetic conditions are discussed and geosynchronous particle data and broadband data from two other stations are presented. Empirical models are employed to predict the location of the plasmapause, and its location is inferred from a knee whistler recorded at Dunedin, New Zealand. These show that Marion Island is in the vicinity of the plasmapause during the event. The event is also compared to chorus observed at similar L after the Halloween storms of 2003. The rarity of the chorus observation is quantified using DEMETER VLF data. The DEMETER data, along with the various ground based VLF measurements, allows us to infer temporal and spatial variations in the chorus source region.

Citation: Delport, B., A. B. Collier, J. Lichtenberger, C. J. Rodger, M. Parrot, M. A. Clilverd, and R. H. W. Friedel (2012), Simultaneous observation of chorus and hiss near the plasmapause, *J. Geophys. Res.*, *117*, A12218, doi:10.1029/2012JA017609.

1. Introduction

[2] Very Low Frequency (VLF) radio waves travel within the plasma filled magnetosphere in the right-hand circularly polarized whistler mode. Chorus is a VLF emission which arises in the magnetosphere from the interaction between background VLF waves and energetic electrons. Chorus consists of a series of short duration ascending (or less often, descending) frequency tones, which are reminiscent of the chirping of a flock of birds [*Sazhin and Hayakawa*, 1992].

[3] Satellite observations show that in space chorus often occurs in two frequency bands, split at 0.5 f_{ce}, where f_{ce} is the local equatorial electron gyrofrequency. Only lower band chorus (that which occurs below 0.5 f_{ce}) is observed on the ground [*Sazhin and Hayakawa*, 1992]. The extent of the magnetosphere in which chorus exists during solar minimum was investigated by *Bunch et al.* [2011], who showed that it was generally confined outside L = 4, with small excursions to lower L in the equatorial plane. They also showed that chorus is found at all Magnetic Local Times (MLTs), but is most prominent in the noon and midnight-dawn sector (albeit over a smaller latitude range), and that, apart from in the dusk sector, chorus activity was found to increase with increasing geomagnetic activity.

[4] In contrast, VLF hiss appears as a uniform broadband emission. There are three varieties of hiss, each with its own spectral properties and occurrence pattern: auroral hiss [*Sazhin et al.*, 1993] observed in the auroral zone, midlatitude hiss observed at midlatitudes outside the plasmasphere, and plasmaspheric hiss observed inside the plasmasphere [*Sazhin and Hayakawa*, 1992]. Plasmaspheric hiss is typically observed at lower frequencies, from several hundred to a few thousand Hz, while midlatitude hiss extends up to more than 10 kHz. Simultaneous observations of chorus and hiss in the same frequency range were first found in GEOS-1 data [*Cornilleau-Wehrlin et al.*, 1978]. Both chorus and hiss fell within the expected 0.05 f_{ce}–0.5 f_{ce} frequency range of chorus.

[5] In order to be observed on the ground, whistler mode waves must travel within ducts, ie: regions of enhanced or depleted plasma density. Unducted whistler mode waves can undergo magnetospheric reflection within the plasmasphere when the local Lower Hybrid Resonance (LHR) frequency is

[1]School of Chemistry and Physics, University of KwaZulu-Natal, Durban, South Africa.
[2]SANSA Space Science, Hermanus, South Africa.
[3]Space Research Group, Department of Geophysics and Space Sciences, Eötvös University, Budapest, Hungary.
[4]Physics Department, University of Otago, Dunedin, New Zealand.
[5]Laboratoire de Physique et Chimie de l'Environnement et de l'Espace, Orléans, France.
[6]Climate Programme, British Antarctic Survey, Natural Environment Research Council, Cambridge, UK.
[7]Los Alamos National Laboratory, Los Alamos, New Mexico, USA.

Corresponding author: B. Delport, School of Chemistry and Physics, University of KwaZulu-Natal, Durban 4000, South Africa.

©2012. American Geophysical Union. All Rights Reserved.
0148-0227/12/2012JA017609

greater than the wave frequency [*Jirícek et al.*, 2001; *Kimura*, 1985]. This typically occurs at an altitude of a few hundred kilometers, within the outer ionosphere. This prevents unducted waves with frequencies lower than LHR frequency from penetrating into the Earth Ionosphere Waveguide (EIWG). Ray tracing models were used by *Inan and Bell* [1977] to investigate the guiding effect of the plasmapause on VLF waves in the magnetosphere. This guiding is very similar to that provided by ducts, and allows VLF waves which propagate close to the inner edge of the plasmapause to be guided down into the EIWG, avoiding reflection from the LHR layer.

[6] Chorus is generated outside the plasmasphere, where growth of whistler mode waves is favorable [*Summers et al.*, 1998]. Chorus is most prevalent in the morning sector, although it can be observed at other local times [*Sazhin and Hayakawa*, 1992]. It is typically associated with substorms, where energetic electrons are injected into the midnight inner magnetosphere, and drift eastward toward dawn under the influence of gradient and curvature drifts. This accounts for the prevalence at dawn. These drifts are dispersive, with higher energy electrons traveling faster. This sometimes causes a gradual increase in the emission frequency with time [*Smith et al.*, 1996; *Collier and Hughes*, 2004].

[7] *Church* [1983] first suggested that chorus may be the source of plasmaspheric hiss, and an observation supporting this idea was discussed by *Parrot et al.* [2004]. *Bortnik et al.* [2008] employed ray tracing models to investigate the propagation of chorus waves in the magnetosphere. Waves were launched with a range of wave normal angles from a point outside the plasmasphere. Only waves with a particular range of wave normal angles were able to penetrate through the plasmapause. The lower damping rates inside the plasmasphere extended the lifetime of these waves, which allowed them to magnetospherically reflect many times, filling the plasmasphere with their energy, generating a wave signature strongly resembling hiss. Using data from two THEMIS satellites, *Bortnik et al.* [2009] presented simultaneous observations of hiss inside the plasmasphere and chorus outside of it, concluding that chorus elements, after crossing the plasmapause and becoming dispersed, smear out to form hiss. These studies appear to provide a plausible explanation for the generation of plasmaspheric hiss.

[8] Early observations associated chorus observations with particle precipitation [*Rosenberg et al.*, 1971; *Foster and Rosenberg*, 1976; *Rosenberg et al.*, 1981]. Doppler shifted cyclotron resonance interaction with whistler mode waves can scatter electrons into the bounce or drift loss cones. When the waves and particles are in resonance, energy is transferred either from the waves to the particles, or visa versa. The direction of net energy flow is determined by the thermal anisotropy of the electron velocity distribution [*Kennel and Petschek*, 1966]. The resonance interaction is thought to occur in the equatorial plane where the energy requirements are minimized. The electron parallel velocity required for resonance is lower when waves travel parallel to the magnetic field lines, which is most often realized with ducted waves [*Tsurutani and Lakhina*, 1997]. With the use of man made VLF transmitters, *Clilverd et al.* [2008] demonstrated that below $L = 1.5$ there was very little evidence of ducted waves. This was attributed to the orientation of magnetic field lines relative to the ionosphere at low L being unfavorable for the trapping of waves. However, at $L > 1.5$, where the magnetic field line configuration was more favorable for the trapping of VLF waves, the vast majority of the wave power was ducted.

[9] *Meredith et al.* [2003] presented results of an analysis looking for favorable regions of the magnetosphere for chorus enhancement, and comparing these to actual chorus observations by CRRES at different geomagnetic activity levels. This revealed that at moderate levels of geomagnetic activity, the dayside region of chorus generation was limited in L and MLT. Additionally, the latitudinal extent of this region extended to latitudes of ~30° North and South on the dayside. A pronounced symmetry between the northern and southern hemisphere chorus generation was also evident.

[10] An interesting chorus event was observed at Palmer, Antarctica ($L = 2.4$) during the recovery phase of the Halloween storms of 2003 [*Spasojevíc and Inan*, 2005]. During this period of extreme geomagnetic activity, the Earth's outer radiation belt became depleted, and the inner radiation belt populated with high energy particles [*Baker et al.*, 2004].

[11] *Golden et al.* [2010] investigated the relationship between the L of the plasmapause (L_{pp}) and chorus received at Palmer. They found that chorus activity peaked at $L_{pp} = 2.6$, when Palmer was just inside the plasmasphere. Further statistical studies of chorus and hiss observations at Palmer were performed by *Golden et al.* [2009, 2011]. The first of these found that chorus and hiss were only observed simultaneously in the local morning. They also found that the majority of simultaneous chorus and hiss occur in different frequency bands. Additionally, these emissions were observed together more frequently when geomagnetic activity was higher. *Golden et al.* [2011] investigated the occurrence rates of chorus and hiss over ten years, from May 2000 to May 2010. They found that chorus was observed only in the morning sector, in the 2–5 kHz frequency range. Hiss was observed at dusk and dawn in the 1–3 kHz range. They also showed that chorus and hiss activity were related to solar cycle variation.

[12] This study presents an unusual terrestrial observation of chorus and hiss at low L. This event is compared to that of *Spasojevíc and Inan* [2005]. Some interesting features of the chorus are linked to the findings of *Bortnik et al.* [2008, 2009]. We present data from several VLF receivers which indicate that chorus generation occurs over a significant longitudinal range. We employ DEMETER data to verify that the event was indeed an uncommon occurrence for this phase of the solar cycle.

2. Observations

[13] On 4 August 2010 chorus was observed at Marion Island (46.9°S 37.1°E, $L = 2.60$, LT = UT + 3) and SANAE IV (71.4°S 2.51°W, $L = 4.32$, LT = UT). The VLF receivers at Marion Island and SANAE IV are crossed loop magnetic antenna, based on the design of the VLF antenna used at Halley, Antarctica [*Bullough and Sagredo*, 1973]. The receivers and preamps are identical. The area of the loops at Marion Island is 5.3 m^2, and have a sensitivity of 2.5×10^{-16} Wm^{-2} Hz^{-1}. The data from these systems are digitized with a sampling frequency of 20 kHz, using 8 bit samples which means the system is sensitive to a range ~42 dB. The system at SANAE IV frequently observes chorus, hiss, whistlers and quasiperiodic emissions. One expects that the system at

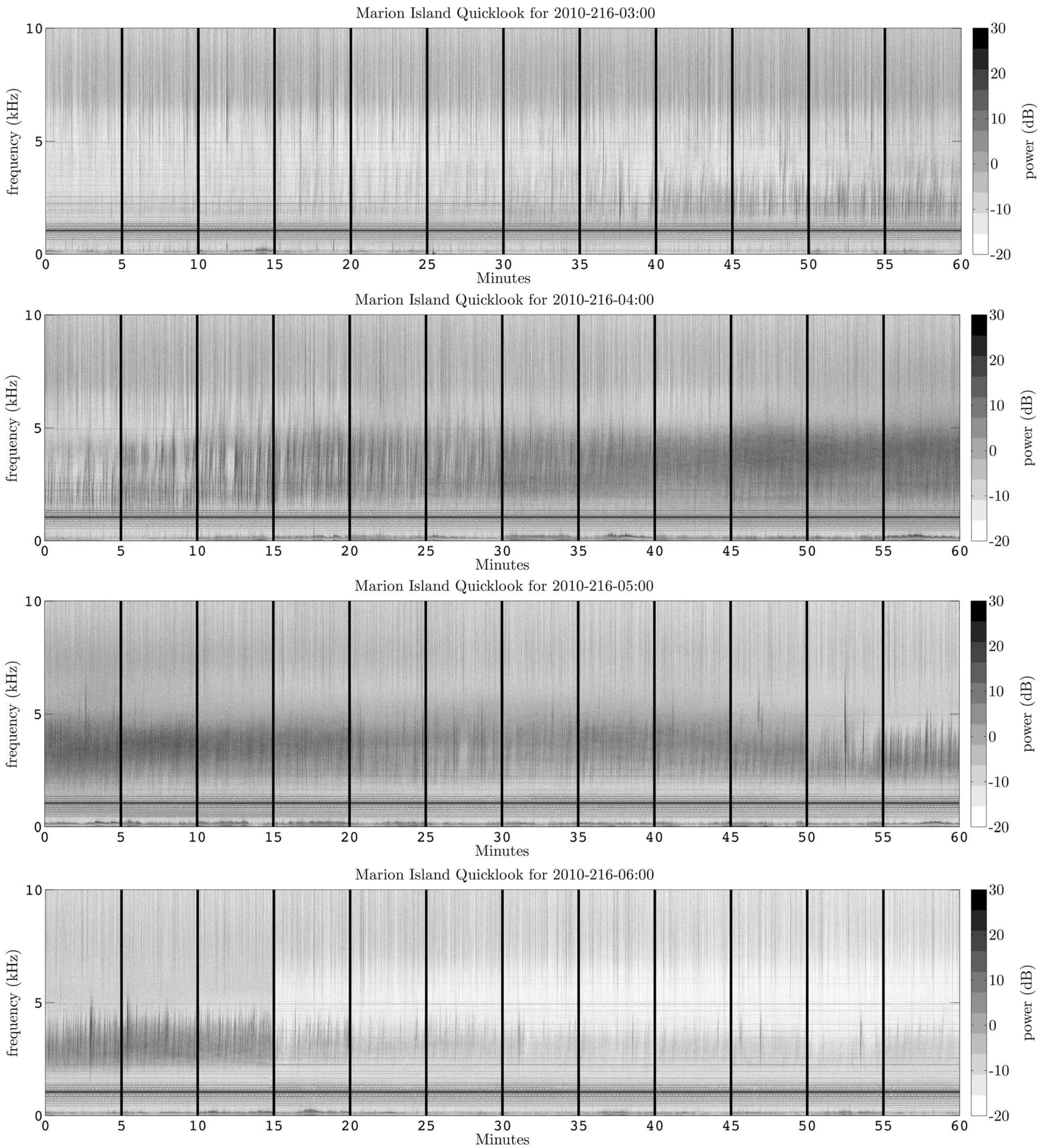

Figure 1. The evolution of chorus at Marion Island over 4 hours from 03:00–07:00 UT on 4 August 2010 with time resolution of 50 ms. Each plot represents 1 hour of data, and each vertical slice represents 1 minute of data sampled every 5 min. The chorus transforms into hiss at 04:30 UT, which evolves to chorus at 05:50. There are changes to the upper boundary of the frequency envelope during the evolution.

Marion Island is similarly capable albeit with a lower sensitivity resulting from smaller loops. The broadband data recording system [*Collier and Hughes*, 2002] allows for signals at frequencies up to 10 kHz to be observed. The system nominally operates in a synoptic mode, recording one minute of data every 5 min. Spectrograms with resolution of 50 ms are shown in Figure 1. The event on 4 August 2010 started at 03:00 UT and persisted until 07:00 UT. The onset time corresponds to local dawn, which is the expected occurrence time for chorus. The spectral structure was not constant throughout the duration of the event. Between 03:00 and 04:00 UT chorus emerged from a quiet background, spanning an initial frequency band of 2–4 kHz. Between 04:00 and 05:00 UT the upper edge of the emission envelope increased to 5 kHz, while

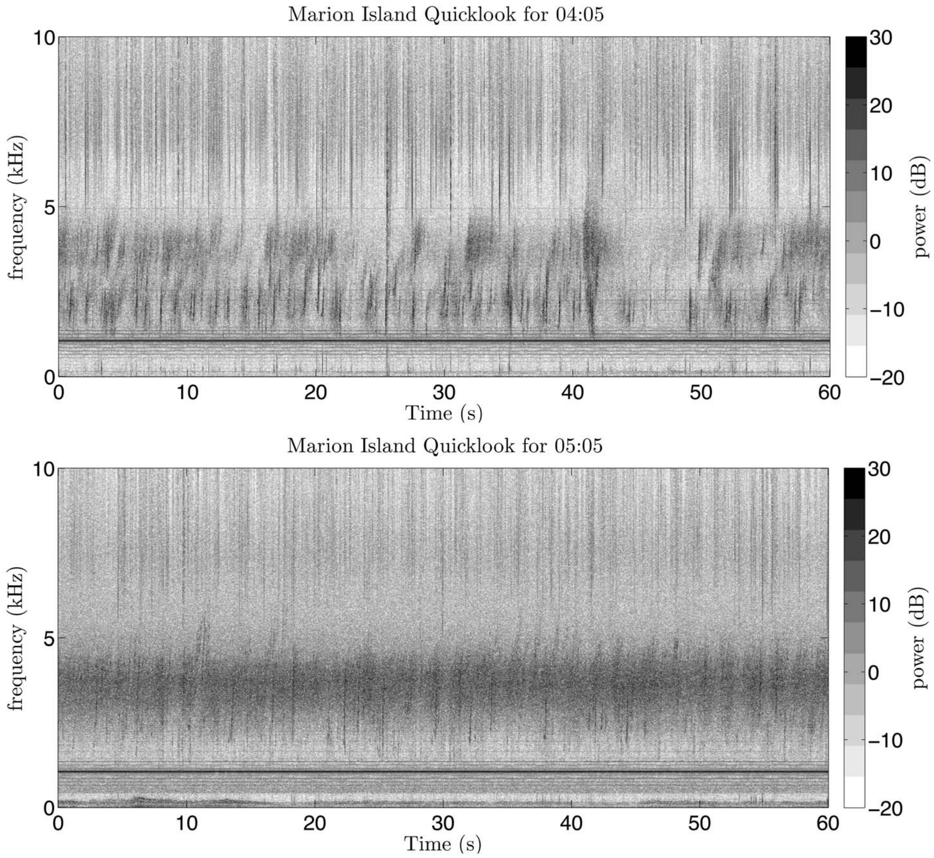

Figure 2. Detailed spectrograms of the (top) chorus (at 04:05 UT) and (bottom) hiss (at 05:05 UT). The structure of the chorus elements is visible in the top panel, and in the bottom panel, one can see that chorus elements are still present beneath the hiss.

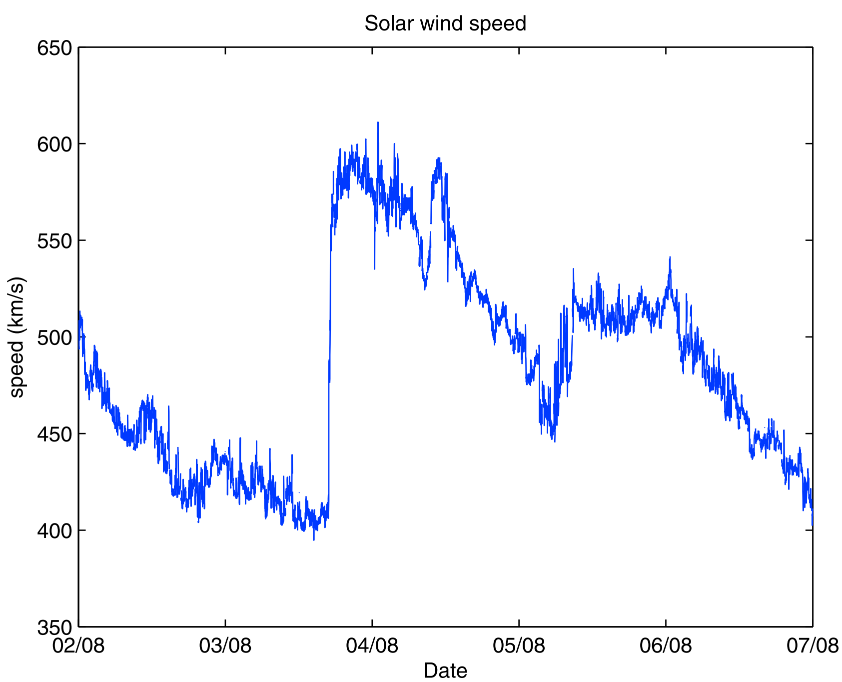

Figure 3. The of the solar wind flow speed as measured by the SWEPAM experiment on board ACE from 2 August to 6 August 2010. There is substantial increase in the measured speed a few hours prior to 4 August 2010.

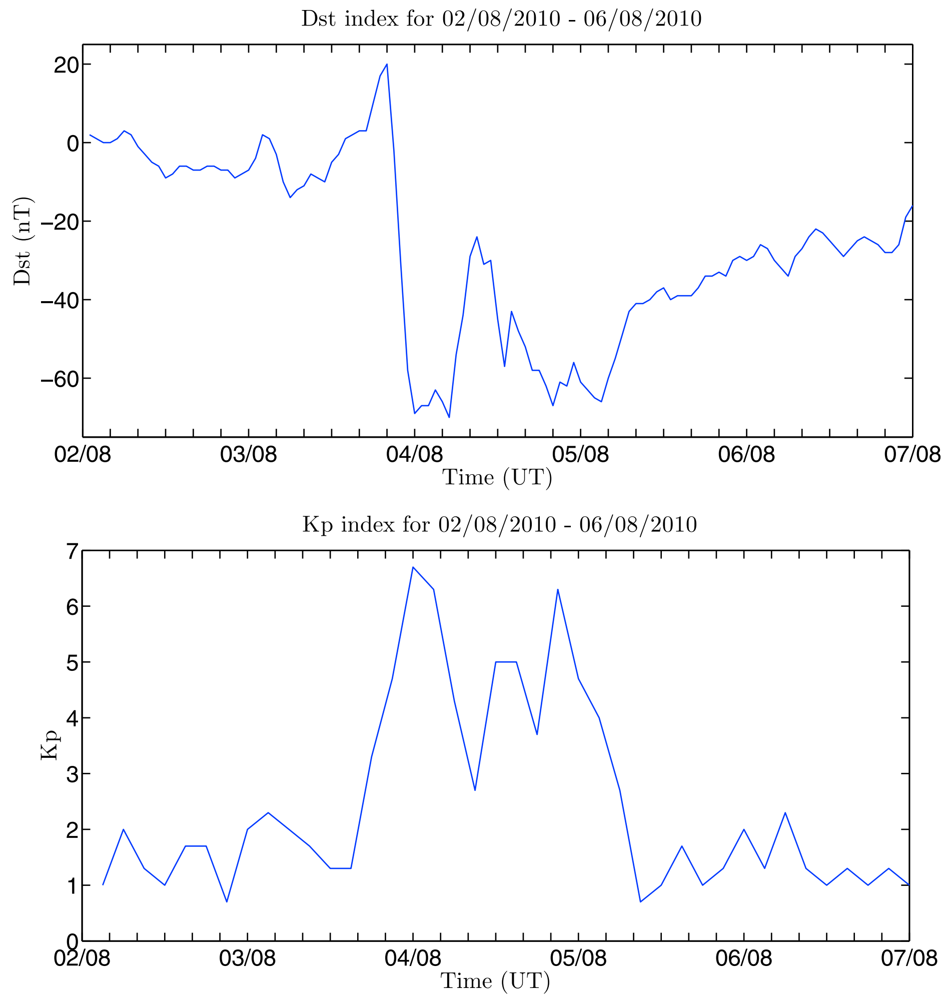

Figure 4. The Dst and K_p indices from 2 to 7 August 2010. The signature of a geomagnetic storm is evident in Dst at 00:00 UT on 4 August 2010, 3 hours before the onset of the chorus at Marion Island. There is a rapid increase in K_p at this time.

the chorus lost structure and became more homogeneous, i.e. hiss-like. This form persisted until approximately 05:50 UT when it reverted back to well-defined chorus with a frequency range of 2–4 kHz. Over the next hour, the emission decreased in intensity and finally faded out completely. Spectrograms showing a more detailed view of the emissions are plotted in Figure 2. The chorus is evident in the minute of data starting at 04:05 UT (Figure 2, top), and hiss at 05:05 UT (Figure 2, bottom). Here the structure of the chorus is clearly shown, and one can see that individual chorus elements are still visible beneath the hiss.

[14] This event was preceded by a geomagnetic storm with onset at 00:00 UT on 4 August 2010, which was driven by a sudden increase in solar wind speed, evident just before midnight on 4 August 2010 data in Figure 3. This resulted in increased dynamic pressure on the Earth's magnetic field, initiating the geomagnetic storm. The intensity of the storm is shown by the Dst and K_p indices in Figure 4. A minimum Dst of −65 nT and peak K_p of 7− were observed. The standard signature of a storm is evident in the Dst plot. The onset of the chorus at Marion Island occurred during the main phase of the storm, and does not extend into the recovery phase. The K_p index peaks at the same time as the Dst index attains its minimum, and remains at elevated levels throughout the day. In comparison, the 2003 Halloween storm was triggered by a Coronal Mass Ejection (CME), and a minimum Dst of −400 nT was observed [*Spasojevíc and Inan*, 2005]. This indicates that the 2010 event was considerably less potent. However, the effects are comparable, with chorus observed at low L in both cases.

[15] During the Halloween event a dramatic reconfiguration of the Earth's outer radiation belts occurred and the CME compressed the magnetosphere, pushing energetic radiation belt particles from $L > 4$ to below $L = 4$. Despite the lower severity of the August 2010 event, such a major reconfiguration was also experienced during the main phase of this storm, with the radiation belt only being restored to its normal configuration during the course of the next few days. This radiation belt reconfiguration is evidenced in the LANL GPS electron flux [*Friedel et al.*, 2008] data plotted in Figure 5. There is a clear depression in counts across all three energy ranges at the time of the rapid increase in geomagnetic activity, and is most evident in the highest energy range (bottom panel, $E > 1.25$ MeV). After this initial depression in the fluxes, there was an enhancement in energetic electron fluxes which persisted for several days after the storm.

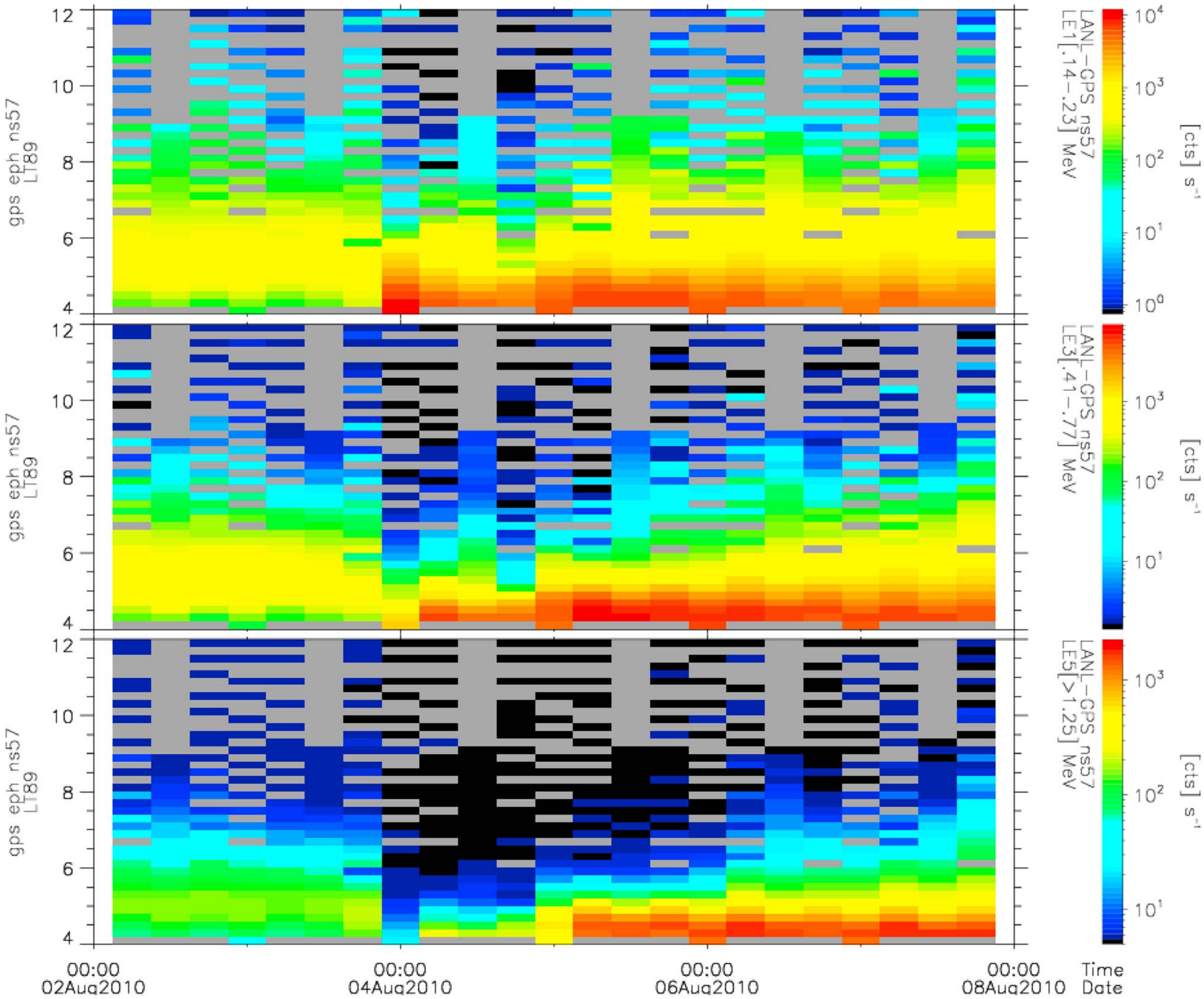

Figure 5. Electron flux data obtained from detectors on LANL GPS satellite NS57 in the range from L = 4–12, in three energy channels. There is a depletion in the radiation levels at the time of the storm onset, and an increase in density at $4 \leq L \leq 5$ for the next few days.

[16] Additional broadband VLF data were also available from Antarctic research stations at SANAE IV and Halley Bay (75.58°S 26.56°W, L = 4.48, LT = UT − 2). The SANAE IV data show chorus developing from 06:00–08:00 UT, later than the chorus at Marion Island. The evolution of the emission at SANAE IV is presented in Figure 6, which shows chorus that is structurally different from that at Marion Island. The time resolution of this spectrogram is the same as that in Figure 1. At SANAE IV the chorus spans a fixed frequency band from 1–2.5 kHz, and at no time is any hiss evident. This hiss is thus generated in a different part of the magnetosphere, and subjected to different resonance conditions.

[17] The Halley Bay VELOX [*Smith*, 1994] data have a much lower time resolution ∼2 min, but still provide useful insight. These data are presented in Figure 7, where the onset of chorus is at around 01:00 UT and spans 2–3.5 kHz. The large onset of activity at 06:00 also occurs in the data from the previous day, before the onset of the geomagnetic storm, and is thus not relevant to the present study. This is useful for providing relative timing and to track the emission generation region.

[18] With observations at three separate receivers it is possible to determine if the MLT of the generation region is changing. The first observation was at Halley Bay at 01:00 UT. The next observation was made at Marion Island at 03:00 UT. Finally, the chorus was observed at SANAE IV starting at 06:00 UT. The locations of these stations and their respective L-shells are shown in Figure 8. From the relative position of Halley Bay and Marion Island, it seems that the chorus source region was moving eastward. However, it is then unusual for the chorus to be observed at Marion Island before SANAE IV, since it lies between Halley Bay and Marion Island. Another explanation is that perhaps the activity observed at Halley is something other than chorus. The low resolution of the Halley data makes it impossible to say with absolute certainty.

3. Results and Discussion

[19] The transformation of the chorus to hiss is of immediate interest since plasmaspheric hiss occurs inside the plasmasphere while chorus is generated outside the plasmasphere.

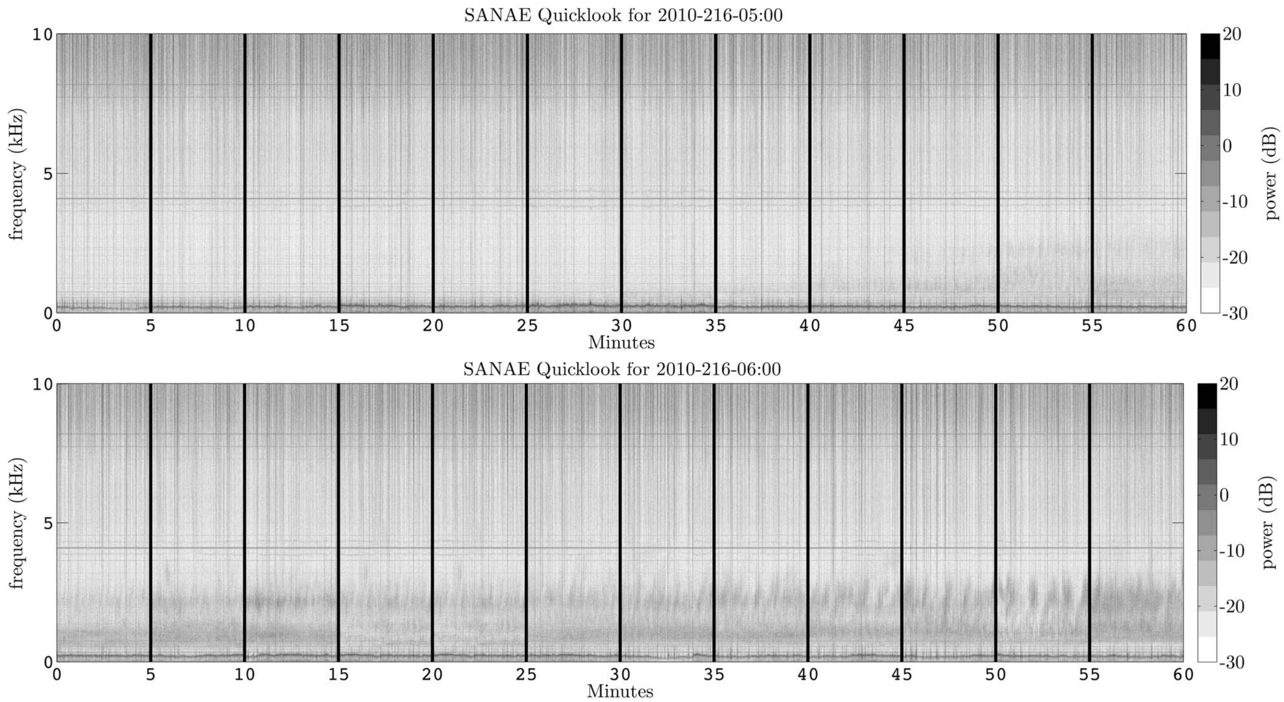

Figure 6. VLF spectrograms at SANAE IV from 05:00–07:00 UT on 4 August 2010. The format is the same as Figure 1. There is chorus for the duration of these spectrograms. This chorus spans a different frequency range, and occurs at a later UT than the Marion Island chorus.

This is strong evidence that Marion Island is in the vicinity of the plasmapause at the time of the event. Both chorus and hiss emissions are able to propagate sub-ionospherically from their respective EIWG entry points to Marion Island. However, the observations were made during daylight hours when sub-ionospheric propagation conditions are not favorable. Thus, with the reduced propagation distance, Marion Island must lie somewhere between their respective source regions, probably close to the plasmapause. No similar transformation in spectral structure is observed at SANAE IV, where the chorus spans a different frequency range, which indicates that the resonant electrons have higher energy or that the generation region for these waves is at higher *L*.

[20] There is a possibility that the hiss observed at Marion Island is in fact not plasmaspheric but rather midlatitude, originating from outside the plasmasphere. This would contradict the above argument for Marion Island's proximity to the plasmapause. If this were the case, then with the plasmapause at higher *L* than Marion Island, midlatitude hiss would originate at an *L* between SANAE IV and Marion Island and should then be visible in the SANAE IV data as well. However, as can be seen from Figure 6, no hiss is observed at SANAE IV, and so we conclude that the hiss is most likely plasmaspheric.

[21] Since chorus is generated outside the plasmasphere, the *L*-value of the plasmapause is an important piece of

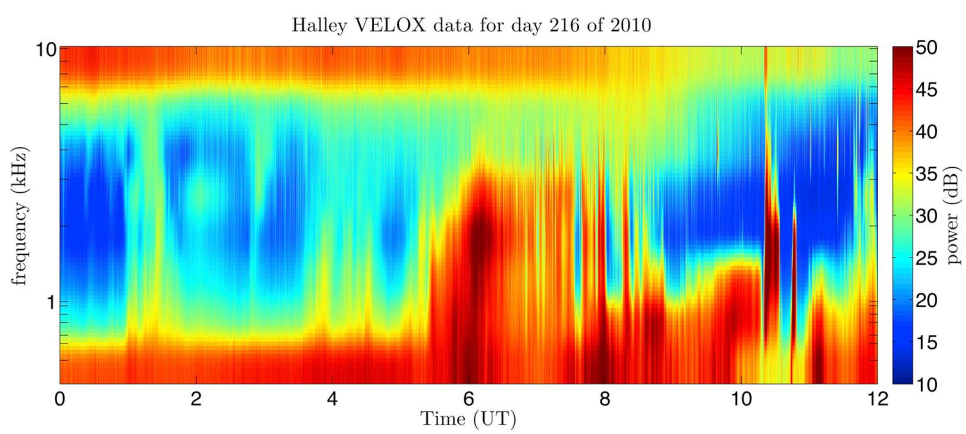

Figure 7. Broadband VLF data obtained at Halley Bay from 00:00–12:00 UT on 4 August 2010 with time resolution of 2 min. There is an onset of activity at 01:00 UT.

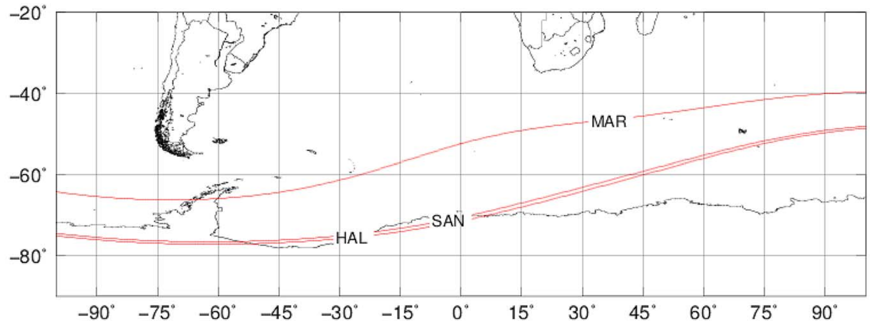

Figure 8. A map showing the relative positions of Halley Bay, SANAE IV and Marion Island as well as their *L*-shells mapped down to the surface of the Earth.

information for this analysis. An initial estimate of L_{pp} was obtained from the simple model of *Carpenter and Park* [1973],

$$L_{pp} = 5.7 - 0.47\,K_{p\max}, \quad (1)$$

where $K_{p\max}$ is the maximal K_p during the preceding 24 hours. This very crude estimate considers a circular plasmapause, which is most accurate in the dawn sector. Using this model with $K_{p\max} = 7-$ yields a value of $L_{pp} = 2.56$, which is slightly lower than the L of Marion Island. There are newer empirical plasmapause models which better reproduce the shape of the plasmapause, including the bulge at dusk [*Carpenter and Park*, 1973]. Recent models, such as that of *Sheeley et al.* [2001] are better able to reproduce this bulge, but this particular model does not include any geomagnetic activity dependence. *Moldwin et al.* [2002] have produced three models derived from CRRES data, each based on a different geomagnetic index, making them more appropriate for this application. For this study, the K_p model was used, which is given by

$$L_{pp} = -0.39(1 - 0.34\cos(\phi - 4.34))K_{p\max} + 5.6(1 + 0.12\cos(\phi - 0.7854)) \quad (2)$$

where ϕ is 2π(MLT/24) and $K_{p\max}$ is the maximal value of K_p obtained in the previous 36 hours. The result of this model is shown in Figure 9. The L-value of Marion Island is represented by the blue circle, and the model result by the red contour. Since the model only depends on $K_{p\max}$, which does not change during the course of the event at Marion Island, this contour is representative of the entire emission period.

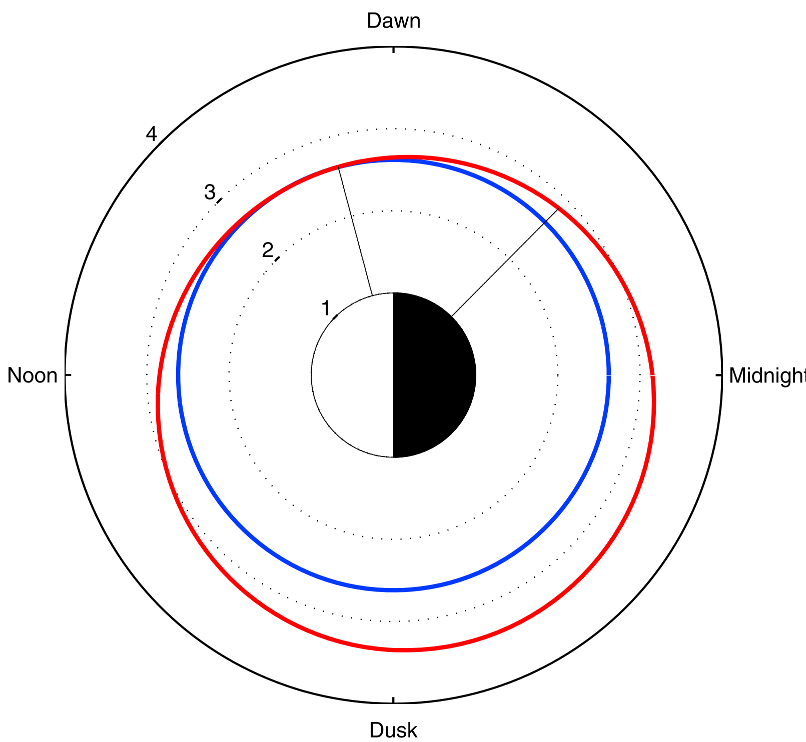

Figure 9. Polar plot of the equatorial plasmapause location obtained from the empirical model in equation (2) (red), and the L-shell of Marion Island mapped into the equatorial plane (blue). The radial black lines show MLT of the period for which chorus was observed at Marion Island. This indicates that the plasmapause was very likely close to Marion Island during the event.

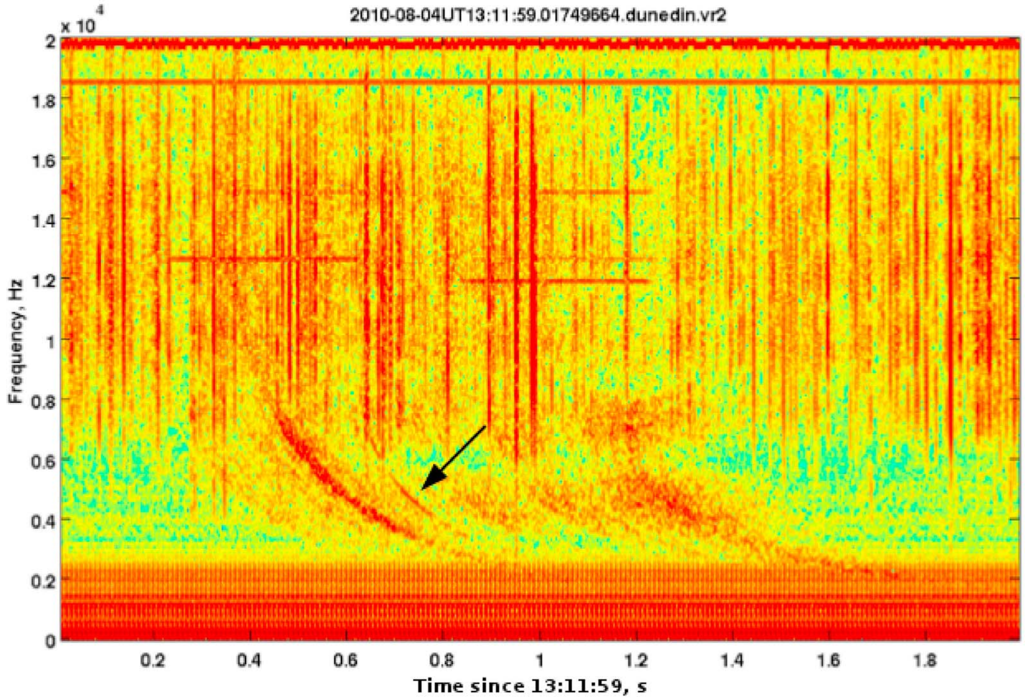

Figure 10. The knee whistler observed at Dunedin on 4 August 2010. The origin of the time axis is 13:11:59 UT. The knee whistler is the well defined trace at approximately 0.8 s, indicated by the arrow.

Marion Island's MLTs at the beginning and end of the event are indicated by the radial lines between midnight and dawn. This plot indicates that Marion Island was very likely just inside the plasmasphere during the event, approaching the plasmapause as the event evolved. It should be noted though that this model result (which could have an error $\sim 1 R_E$) is not as reliable as a direct measurement.

[22] A knee whistler observed on 4 August 2010 at Dunedin, New Zealand (45.78°S 170.47°E, $L = 2.7$), allows a direct estimate of the plasmapause location [*Carpenter*, 1963]. A knee whistler is one for which some of the whistler traces have traveled inside the plasmasphere, and others outside of it. These two groups experience significantly different plasma densities, and this is reflected in their dispersion. Since a knee whistler has traveled virtually along the plasmapause, it can be used to determine L_{pp}. In the spectrogram of Figure 10, the knee whistler occurs at $t = 0.8$ s (identified by the arrow). Analysis by the Automatic Whistler Detector and Analyser (AWDA) [*Lichtenberger et al.*, 2008, 2010] identifies this as a knee whistler since it corresponds to an equatorial electron density of 227 cm^{-3}, while the other whistlers in the group show an equatorial electron density of 734 cm^{-3}. L_{pp} was determined using the AWDA, and it was found that $L_{pp} = 3.5$ at 13:12 UT at Dunedin, which corresponds to around 00:12 LT. The AWDA uses a Vertical Trace Transform (VTT) for extracting parameters from whistlers. This technique is still in development, and so we employed the more traditional whistler scaling to determine L_{pp} from the knee whistler [*Lichtenberger*, 2009], which has the benefit of providing the uncertainty range for the result. The results from this method are L_{pp} 3.542 $\pm$ 0.085, and equatorial electron density of 217 $\pm$ 7 cm^{-3}. Thus it appears that the values obtained using VTT fall within 1σ for L_{pp} and 2σ for the equatorial number density. For simplicity, we will use $L_{pp} = 3.5$ from here on. We argue that since this observation is made 6 hours later than that of the Marion Island chorus (at $\sim$13:00 UT), and we expect the plasmasphere to have relaxed somewhat since 07:00 UT, that the value of $L_{pp} = 3.5$ is an upper bound on L_{pp} during the chorus observed at Marion Island.

[23] Both the model depicted in Figure 9, and the value of L_{pp} determined from the knee whistler analysis indicate that Marion Island was within the plasmasphere during this event. Since chorus is generated outside the plasmasphere, one might naively expect chorus observations only during periods where the receiver is outside the plasmasphere. However, since VLF waves can propagate sub-ionospherically for significant distances, the observation of chorus is possible for ground stations located inside the plasmasphere but close to the plasmapause. This is not an uncommon occurrence though, recalling that *Golden et al.* [2010] reported that chorus observation at Palmer station was most probable when the receiver was just inside the plasmapause. Additionally, one would expect that hiss originating from inside the plasmapause would not be able to penetrate to the ground, due to reflection at the LHR frequency and at the ionospheric boundary. The plasmapause can guide these hiss emissions to the ground, if the waves are close enough to it. The waves can then propagate within the EIWG to the receiver, which might be inside or outside the plasmasphere, provided the receiver is close enough to the plasmapause. For both of these situations, the question remains: how "close" is close enough?

[24] In Figure 11 circles at distances of 400 and 900 km from Marion Island (blue star) are plotted, as well as contours at $L = 2.60$ (the L of Marion Island), 3.00 (an intermediate L), and 3.50 (the upper bound of L_{pp}). This shows that the AWDA determined value of L_{pp} is as close as 900 km to Marion Island. It is well known that, due to the low

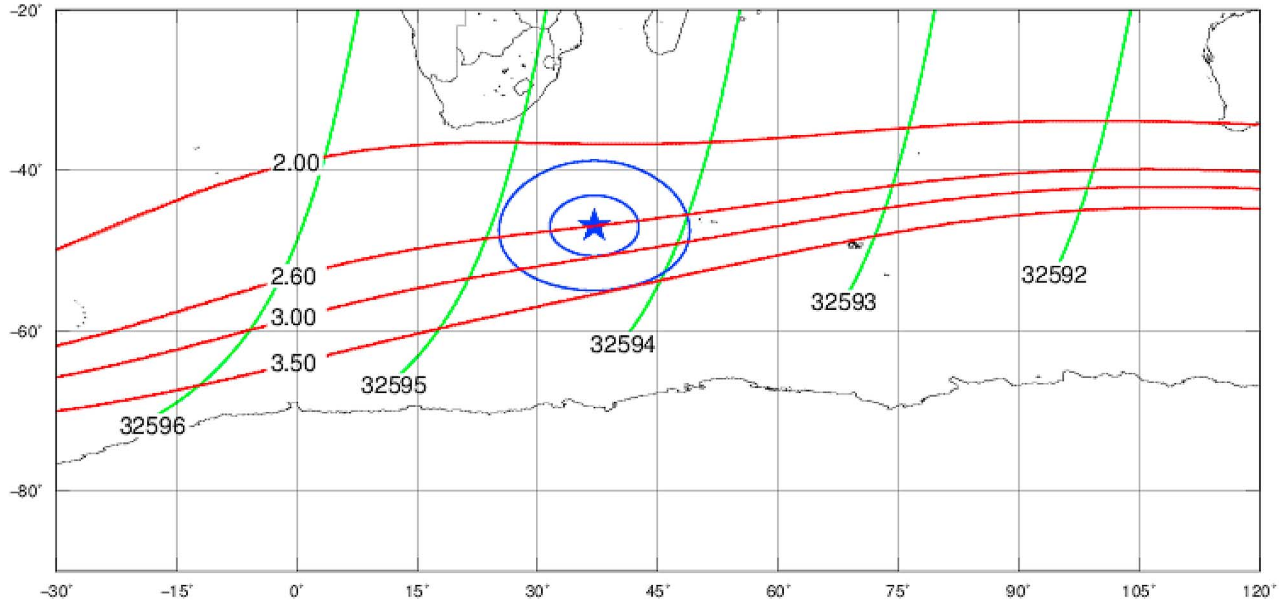

Figure 11. The location of Marion Island plotted as a blue star. The 2 blue circles have a radius of 600 and 1200 km respectively. L-shell contours are plotted at L = 2.00, 2.60, 3.17 and 3.91. The L = 3.91 shell intercepts the 1200 circle, while the L = 2.00 field line is the lower boundary of chorus extent. The path of five DEMETER half orbits which occurred from an hour before, to an hour after the observations at Marion Island and SANAE IV are plotted in green.

attenuation of ~10 dB/Mm [*Barr et al.*, 2000] in the EIWG, VLF waves can travel sub-ionospherically for thousands of kilometers. The emissions shown in Figure 1 are ~30 dB above the background, which would allow for these waves to propagate at least 3000 km. We thus propose that 900 km between the receiver and the plasmapause is surely close enough.

[25] Our event is quite similar to that described by *Spasojevíc and Inan* [2005]. In both cases chorus was observed at low latitude locations which have $L < L_{pp}$ during quiescent conditions. The chorus onset occurs during the main phase of a storm where the plasmapause is pushed inward toward the observing station, and persists into the recovery phase. Both events were observed in the midnight-dawn sector and were accompanied by some form of hiss. There are, however, some significant differences. The 2003 event occurred during solar maximum, a period when the Sun was extremely active, while the 2010 event occurred near the end of a prolonged period where the Sun was unusually quiet. The 2003 chorus persisted for 3 days, while the 2010 event lasted less than one day, but this can probably be attributed to the higher activity levels in 2003. Although both events exhibited hiss, the structure of the hiss was different. The 2003 hiss (described as midlatitude hiss by *Spasojevíc and Inan* [2005]) spanned a larger frequency range than the chorus, and individual chorus elements were visible on top of the hiss. During the 2010 event, the hiss spanned the same frequency range as the chorus, and chorus elements were only visible toward the lower end of the spectrum.

[26] There is significance in the fact that the chorus and hiss observed at Marion Island span the same frequency range. Recent studies [*Bortnik et al.*, 2008, 2009; *Wang et al.*, 2011] have hypothesized that chorus outside the plasmasphere may generate plasmaspheric hiss. *Bortnik et al.* [2009] simultaneously observed chorus outside the plasmasphere and hiss inside of it on two THEMIS satellites which were on either side of the plasmapause. These emissions were found to be in the same frequency range. This observation supported the earlier modeled results of *Bortnik et al.* [2008]. Chorus and hiss are often observed simultaneously at low L, but for them to occur in the same frequency band is uncommon [*Golden et al.*, 2009]. In contrast, the Marion Island chorus and hiss do occur in the same frequency band (as shown in Figure 1), and hence this is a ground based observation supporting the hiss generation theory of *Bortnik et al.* [2008]. The chorus originates from outside the plasmasphere, and has generated plasmaspheric hiss inside the plasmasphere. Our data also indicates that this conversion can take of the order of minutes to occur, which may reflect the complexity of the chorus waves gaining access to the plasmasphere (i.e. that chorus does not always enter the plasmasphere). The simulations of *Bortnik et al.* [2008] showed that only chorus waves with certain wave normal angles are able to penetrate through the plasmapause, which suggests to this complexity. As discussed above, the plasmaspheric hiss is allowed to pass through the ionosphere by the strong guiding provided by the plasmapause.

[27] Alternatively, our observations might be more like those of *Santolík et al.* [2009] who showed a case of chorus and hiss both being generated in the same region, in the equatorial plane near L = 4.25. They suggested that both chorus and hiss were independently generated in roughly the same region. Both emissions were also found to have large wave normal angles, meaning that they could propagate across magnetic field lines, to lower or higher L shells. One thing to note about these observations is that the chorus and hiss seem to be independent of each other, while our observations show that the hiss is superimposed on top of

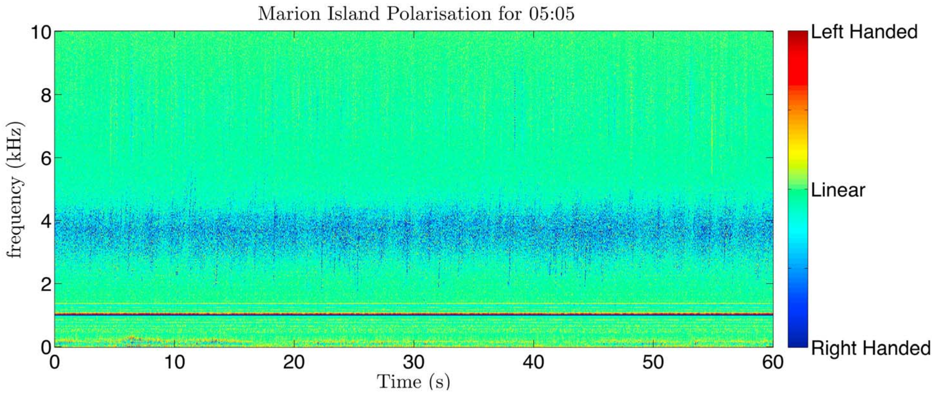

Figure 12. Polarization of the signal received at Marion Island for the minute 05:05 UT. Note the strong right handed polarization of both the chorus and the hiss, indicating a nearby entry into the EIWG.

chorus (as shown in Figure 2). This might mean that the source regions of the chorus and hiss are distinct. We have also shown above that while chorus is observed at higher *L* at SANAE IV, no hiss is evident there. For these reasons we propose that we are indeed seeing the conversion of chorus to hiss inside the plasmasphere.

[28] Measurements from crossed loop antennas can be used to determine the polarization of the signal. One method for doing this with digitally recorded VLF data is described in *Manninen* [2005]. When VLF waves enter the EIWG, they maintain their polarization. When traveling through the EIWG, the polarization of the waves changes, becoming more linearly polarized. *Shimakura et al.* [1986] found that whistlers which entered the EIWG near the receiver were strongly right hand circularly polarized, while those which entered the EIWG further away, were almost completely linearly polarized.

[29] Calculations of the polarization of the received waves allows one to draw conclusions about how far away the emissions are entering the EIWG. We have calculated the polarization of the waves received at Marion Island for the minute of data starting 05:05 UT. This corresponds with the amplitude spectrogram in Figure 2 (bottom). The polarization data are shown below in Figure 12. It is clear that both the chorus and hiss observed at Marion Island are strongly right hand circularly polarized. We can thus conclude that both of these emissions are entering the EIWG close to Marion Island, and that the plasmapause is thus probably close to Marion Island at this time.

[30] The DEMETER satellite [*Berthelier et al.*, 2006] is in a quasi Sun-synchronous low Earth orbit (~700 km), which passes over the same geographical region at roughly the same time each day. The paths of five half orbits which occur just before, during and after the chorus observations are plotted in Figure 11. These half orbits begin at a position east of Marion Island and move westward until they are well west of Marion Island. Figure 13 displays VLF spectra from the ICE instrument on DEMETER, for the 5 half orbits discussed above. The vertical dotted lines show the *L* value of Marion Island in both hemispheres, and the horizontal dotted lines enclose the 2–5 kHz range. Using these data one is able to determine the extent of the chorus generation region in both longitude and *L*. One can see enhanced VLF activity in the vicinity of Marion Island in half orbits 32594 and 32595. During half orbit 32594, the DEMETER satellite switched into burst mode while within the region where chorus was observed in the southern hemisphere. These broadband data are plotted in Figure 14, and clearly shows that chorus was occurring. We have confined the values of dB used to a range close to the peaks observed in Figure 13.

[31] A statistical approach was used in the analysis of the DEMETER data in an effort to establish that the observed chorus is not a regularly occurring phenomenon in this longitude and *L*-range, during this period of the solar cycle. This is the first time that the system at Marion Island has recorded VLF chorus since it was commissioned in early 2007. *Golden et al.* [2009, 2011] showed that chorus and hiss are frequently observed at L = 2.4 at Palmer station. Their results, however, show that chorus and hiss occurrence rates are minimized during solar minimum, but that some observations of chorus were made during 2010. We thus wish to quantify the rarity of chorus at Marion Island for a period around the event. Data from 215 DEMETER half orbits, from April to September 2010 were used in the analysis. The first step in doing this was to generate an average spectrogram (μ) from the DEMETER data. This was done by obtaining data from many half orbits which occur at the same time of day and in the same geographic region, thereby eliminating any MLT or LT dependence. Spectrograms for each of these were then generated and the arithmetic average, μ, of these spectrograms was computed. The average was used to determine the residual of a given spectrogram X_i by calculating $X_i - \mu$, which indicates to what extent a particular X_i differs from the norm. We then proceeded to calculate a quantitative measure of the statistical significance of the chorus observed at Marion Island using normalized residuals [*Hogg and Tanis*, 1989, p. 182] with:

$$z_i = \frac{X_i - \mu}{\sigma}, \tag{3}$$

where σ is the standard deviation of the spectrograms. The collection of these z-values can be used to infer a p-value for the data. The p-value is defined as the probability of obtaining a result at least as extreme as a given result from a set of randomly distributed data. For this analysis, it should be thought of in terms of a 2D spectrogram, where each pixel of the spectrogram transforms to a p-value for that half orbit.

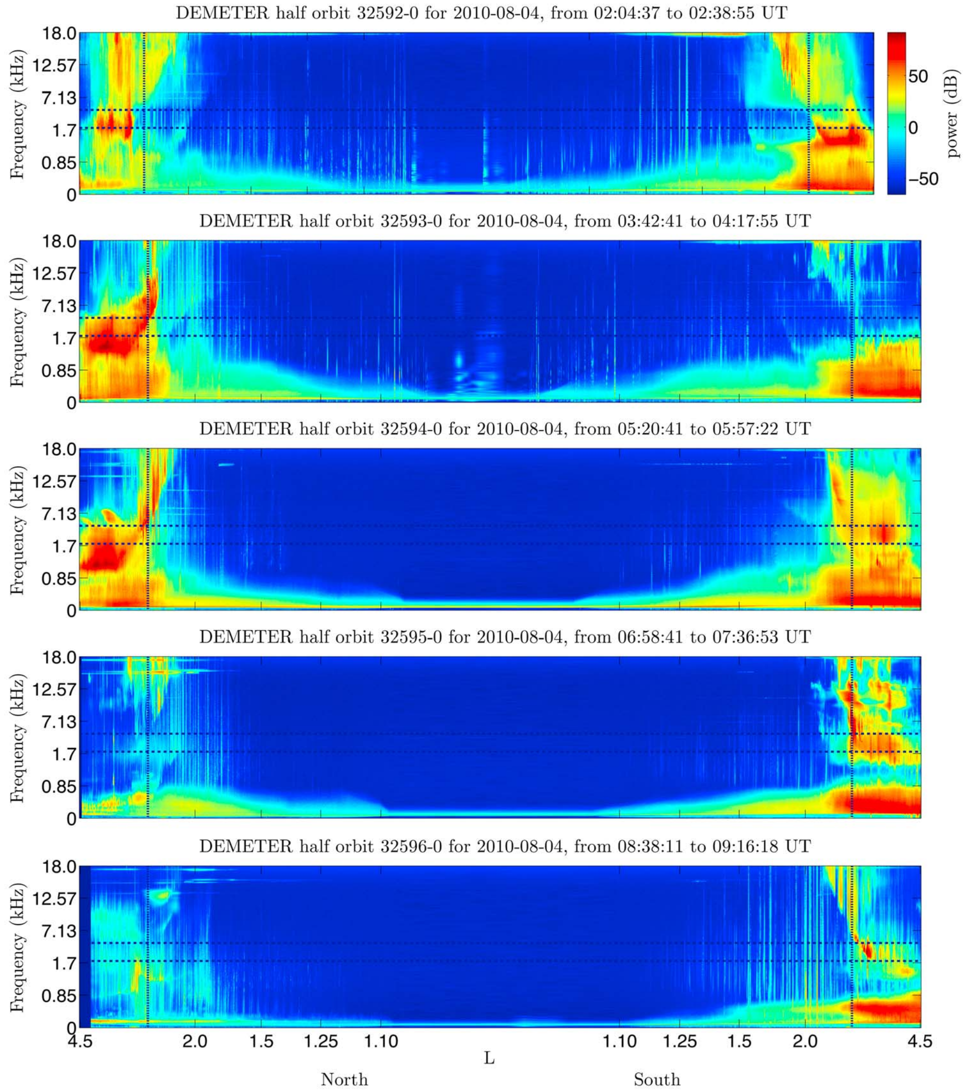

Figure 13. Broadband VLF data from the 5 descending DEMETER half orbits shown in Figure 11. The vertical dotted lines are the L-value of Marion Island ($L = 2.60$) in both hemispheres, and the horizontal dotted lines represent the frequency envelope of the chorus observed on Marion Island.

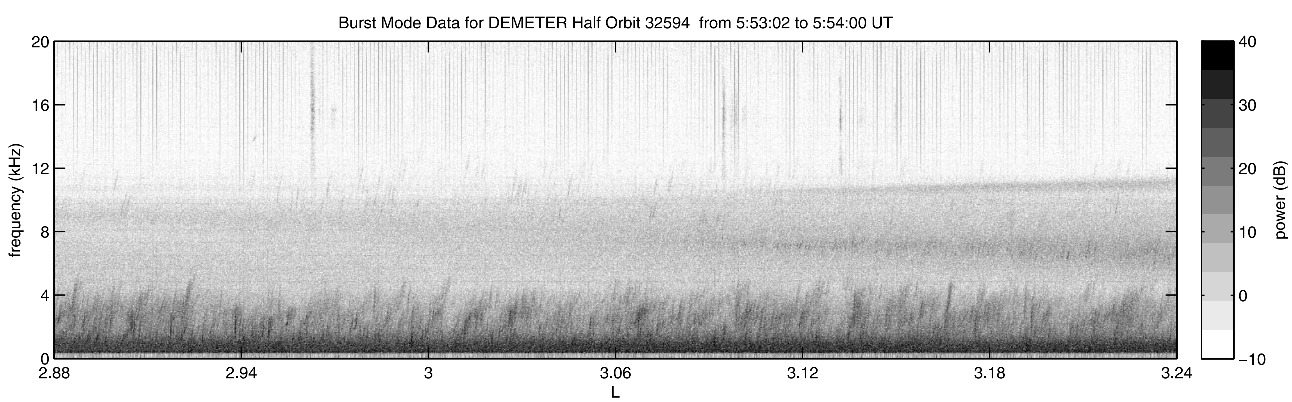

Figure 14. Burst mode VLF data from DEMETER satellite half orbit 32594 which shows chorus being observed. This data is for a one minute period while the satellite was in the southern hemisphere. The position of this spectrogram relative to those plotted in Figure 13 can be inferred from the L-values.

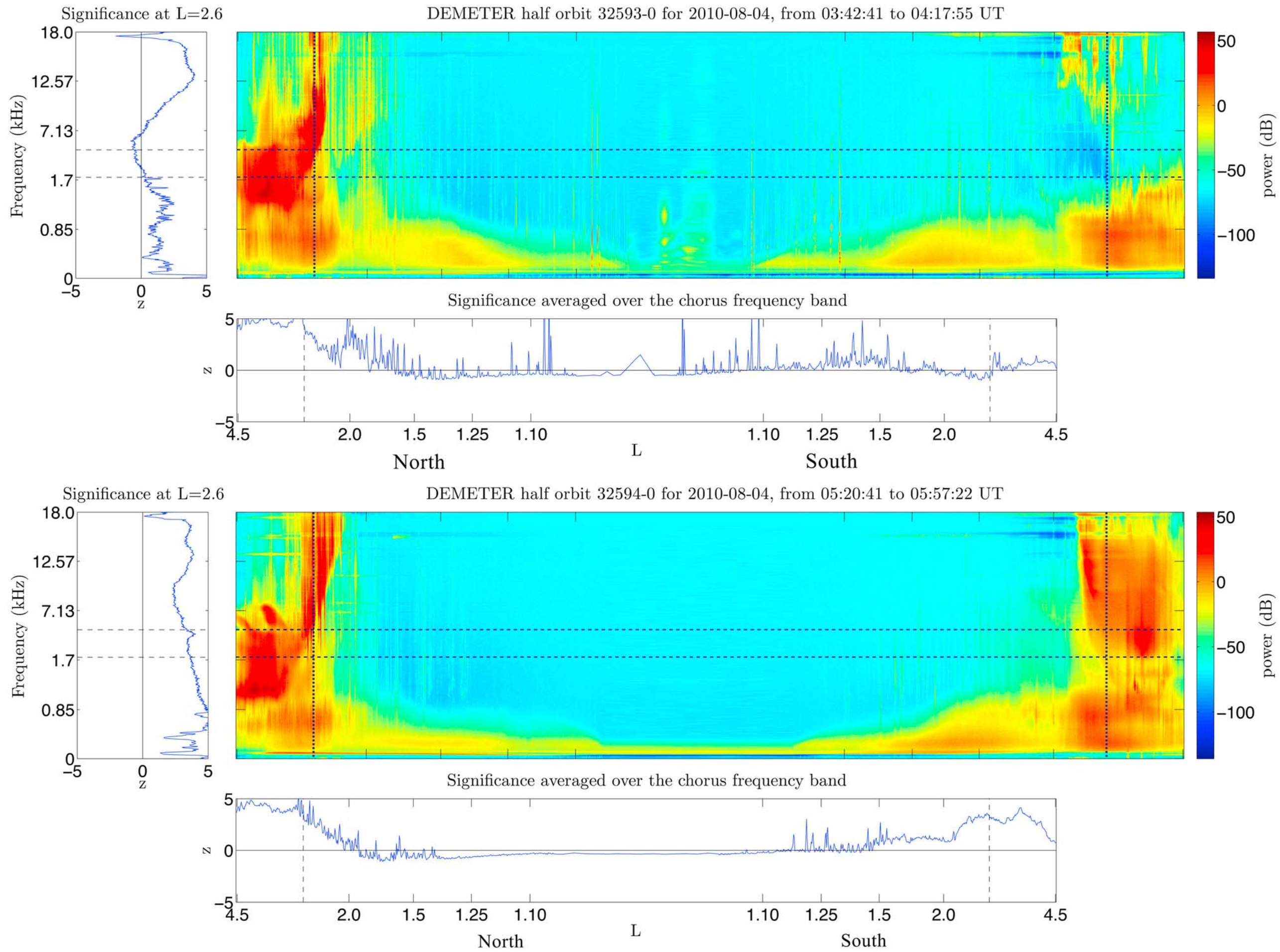

Figure 15. Residual for descending DEMETER half orbits 32593 and 32594. The left hand plots show the z-value obtained at the magnetic latitude of Marion Island. The bottom plots show the z-value averaged over 2–5 kHz. The z-value is large during periods of high chorus activity, and small during periods of no chorus.

A $p \leq 0.05$ indicates a result significant at the 5% level and corresponds to $|z| \geq 1.96$ [*Hogg and Tanis*, 1989, p. 613]. In Figure 15 the normalized residuals of DEMETER half orbits 32593 and 32594 are plotted.

[32] Half orbit 32593 (Figure 15, top) shows no chorus activity in the vicinity of Marion Island. The z-value obtained for this half orbit in the vicinity of Marion Island is close to zero, and is not of statistical significance. In other words, this level of activity is commonly observed in the data. On the other hand, half orbit 32594 (Figure 15, bottom) shows intense chorus activity in the vicinity of Marion Island, and the associated z-value is $\gg 2$, which indicates a high statistical significance. This tells us that chorus is not frequently observed in the data (in $\ll$5% of the data).

[33] The effectiveness of calculating z-values is highlighted in the differences between Figures 15 (top) and 15 (bottom). The z-value is $\sim$0 during periods of little or no chorus activity, while it drastically increases when chorus is present. This technique would be useful for analogous studies in other broadband data sets, either ground based or in situ.

[34] The DEMETER data also allow one to view the VLF spectra across a range of L-values, while the MLT is slowly changing. The VLF spectra are most clearly shown in Figure 16, where the residuals of descending half orbits 32592–32596 are plotted. Comparing these to Figure 11, it is apparent that most of the VLF activity in the chorus and hiss frequency range is confined to the region poleward of L = 2.00 (red curve in Figure 11). The southern hemisphere VLF activity is most intense in half orbits 32594 and 32595, which are those closest to Marion Island. This indicates that the generation region is localized near Marion Island, at $L > 2$ for the duration of the VLF activity.

[35] Another interesting observation from Figure 16 is the apparent asymmetry in the chorus activity between the two hemispheres. In half orbits 32592, 32593 and 32594 there is chorus in the northern hemisphere. However, in the southern hemisphere there is chorus in half orbits 32592 and 32594, and not 32593. It appears as though the satellite has moved through some gap in the chorus generation region. This asymmetry is not expected given the nature of chorus generation (and also based on evidence from *Meredith et al.* [2003]). We propose three possible reasons for this asymmetry:

[36] 1. A half orbit is $\sim$45 min for DEMETER, and there is thus some delay between observations at the top and bottom of the half orbit. This time delay is long enough for chorus generation to switch on or off before reaching the

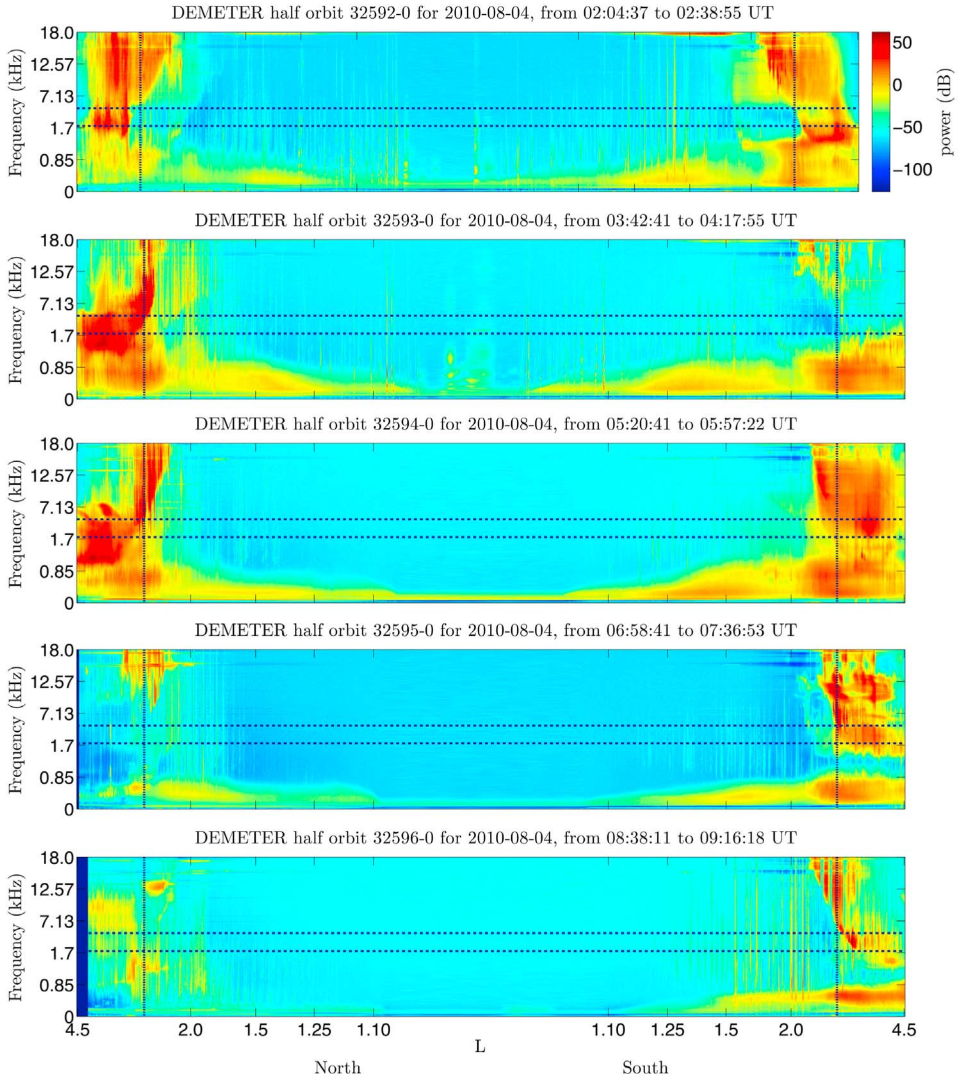

Figure 16. Residuals after a subtraction of the mean of the DEMETER data presented in Figure 13. The chorus is much more evident in these plots. The vertical lines show the *L*-value of Marion Island in both hemispheres. The two horizontal lines show the frequency range 2–5 kHz.

opposite end of the field line. One might, however, discount this reason since the chorus in the northern hemisphere persists for 3 half orbits.

[37] 2. DEMETER does not orbit along magnetic meridians, and so the top and bottom of the half orbit are separated in magnetic longitude. The satellite can thus move out of, or into the chorus generating region along a single half orbit.

[38] 3. The electrons require positive thermal anisotropy for wave growth. It is possible that conditions were such that the southward traveling particles (those resonating with northward traveling waves) had negative anisotropy. Upon mirroring in the southern hemisphere, $T_{\|}$ was reduced in the system as particles were lost by collisions in the neutral atmosphere, leading to positive anisotropy on the northward trip (resonance with southward traveling waves). This allows for enhancement of the southward traveling waves while reducing the anisotropy in the system, and they remained so after the next mirror in the northern hemisphere.

[39] The third reason may seem like a rather convenient set of circumstances, but Marion Island lies eastward of the South Atlantic Magnetic Anomaly (SAMA). This results in particles penetrating to a greater depth in the southern hemisphere (and hence having a larger bounce loss cone) than in the northern hemisphere. This serves to reduce $T_{\|}$ only on the southern hemisphere bounce.

4. Conclusion

[40] VLF chorus observed at Marion Island on the 4 August 2010 was investigated. This was compared to a similar event at Palmer which occurred in 2003 after an intense geomagnetic storm. The 2010 event occurred after a much smaller geomagnetic storm. The geomagnetic activity of the 2003 event compressed the plasmapause to an *L*-value lower than Palmer's *L*-value. The 2010 event is observed while Marion Island is close to, but inside the plasmapause.

[41] This proximity to the plasmapause makes for a remarkable observational opportunity. VLF emissions from both inside and outside the plasmasphere are able to propagate to Marion Island, giving a continuous view of these two regimes. This allowed the simultaneous observation of chorus and plasmaspheric hiss. A similar observation was made by *Bortnik et al.* [2009] using two THEMIS satellites positioned on either side of the plasmapause. Our observations at Marion Island support their findings that chorus penetrating into the plasmasphere is the source of plasmaspheric hiss.

[42] Data from two other stations were used to track the motion of the chorus generation region. The location of the plasmapause was determined with the use of two models based on geomagnetic activity. A serendipitous observation of a knee whistler at Dunedin, New Zealand, allow for a more direct estimate of the location of the plasmapause. There was significant disparity between the value of L_{pp} obtained from the knee whistler analysis and the modeled result. The difference can be attributed to inaccuracies of the model, as well as the knee whistler being observed later in the day.

[43] We have also used DEMETER VLF data to determine the size of the generation region. An averaging technique was used to determine uncommon features in the VLF data, and a direct measure of the statistical significance of particular features in the data was obtained. Using this analysis allowed for a quantitative measure showing that chorus is not commonly observed in the vicinity of Marion Island. This technique can be directly applied to any other spectrogram type data sets.

[44] Marion Island was in a favorable position for viewing this event. The L value of Marion Island puts it close to where one might expect to find the plasmapause during disturbed periods, which acts a dividing layer between two VLF generation regimes in the magnetosphere. Additionally, we have discussed how the plasmapause itself may have played a role in guiding plasmaspheric emissions through the LHR reflection layer. Marion Island's location just eastward of the SAMA also means that electrons drifting toward Marion Island have just passed through the SAMA, which would cause dramatic reconfigurations to their velocity distribution.

[45] This unusual observation was made possible by the particular level of geomagnetic activity. Higher levels of activity would have resulted in only chorus being observed, as was the case for Palmer. However, sufficient activity was required to shift the plasmapause close enough to Marion Island to allow for the sub-ionospheric propagation of hiss to the receiver. This is a rather unique set of circumstances.

[46] **Acknowledgments.** The authors thank J. J. Berthelier the PI of the DEMETER electric field experiment for the use of their data. The research leading to these results has received funding from the European Community's Seventh Framework Programme (FP7/2007–2013) under grant agreement 263218.

[47] Robert Lysak thanks the reviewers for their assistance in evaluating this paper.

References

Baker, D. N., S. G. Kanekal, X. Li, S. P. Monk, J. Goldstein, and J. L. Burch (2004), An extreme distortion of the van allen belt arising from the halloween solar storm in 2003, *Nature*, *432*, 878–881.

Barr, R., D. Jones, and C. Rodger (2000), ELF and VLF radio waves, *J. Atmos. Sol. Terr. Phys.*, *62*(17–18), 1689–1718, doi:10.1016/S1364-6826(00)00121-8.

Berthelier, J. J., et al. (2006), ICE, the electric field experiment on DEMETER, *Planet. Space Sci.*, *54*(5), 456–471, doi:10.1016/j.pss.2005.10.016.

Bortnik, J., R. Thorne, and N. Meredith (2008), The unexpected origin of plasmaspheric hiss from discrete chorus emissions, *Nature*, *452*(7183), 62–66, doi:10.1038/nature06741.

Bortnik, J., W. Li, R. M. Thorne, V. Angelopoulos, C. Culley, J. Bonnel, O. L. Contel, and A. Roux (2009), An observation linking the origin of plasmaspheric hiss to discrete chorus emissions, *Science*, *324*, 775–778, doi:10.1126/science.1171273.

Bullough, K., and J. L. Sagredo (1973), VLF goniometer observations at Halley Bay, Antarctica I. the equipment and the measurement of signal bearing, *Planet. Space Sci.*, *21*(6), 899–912, doi:10.1016/0032-0633(73)90138-4.

Bunch, N. L., M. Spasojevic, and Y. Y. Shprits (2011), On the latitudinal extent of chorus emissions as observed by the Polar Plasma Wave Instrument, *J. Geophys. Res.*, *116*, A04204, doi:10.1029/2010JA016181.

Carpenter, D. L. (1963), Whistler evidence of a knee in the magnetospheric ionization density profile, *J. Geophys. Res.*, *68*(6), 1675–1682, doi:10.1029/JZ068i006p01675.

Carpenter, D. L., and C. G. Park (1973), On what ionospheric workers should know about the plasmapause-plasmasphere, *Rev. Geophys. Space Phys.*, *11*(1), 133–154.

Church, S. (1983), On the origin of plasmaspheric hiss: Ray path integrated amplification, *J. Geophys. Res.*, *88*(A10), 7941–7957, doi:10.1029/JA088iA10p07941.

Clilverd, M. A., C. J. Rodger, R. Gamble, N. P. Meredith, M. Parrot, J. J. Berthelier, and N. R. Thomson (2008), Ground based transmitter signals observed from space: Ducted or nonducted, *J. Geophys. Res.*, *113*, A04211, doi:10.1029/2007JA012602.

Collier, A. B., and A. R. W. Hughes (2002), Digital VLF recording and analysis system for SANAE IV, *S. Afr. J. Sci.*, *98*, 547–550.

Collier, A. B., and A. R. W. Hughes (2004), Modelling substorm chorus events in terms of dispersive azimuthal drift, *Ann. Geophys.*, *22*, 4311–4327, doi:10.5194/angeo-22-4311-2004.

Cornilleau-Wehrlin, N., R. Gendrin, F. Lefeuvre, M. Parrot, R. Grard, D. Jones, A. Bahnsen, E. Ungstrup, and W. Gibbons (1978), VLF electromagnetic waves observed onboard GEOS-1, *Space Spi. Rev.*, *22*(4), 371–382, doi:10.1007/BF00210874.

Foster, J. C., and T. J. Rosenberg (1976), Electron precipitation and VLF emissions associated with cyclotron resonance interactions near the plasmapause, *J. Geophys. Res.*, *81*(13), 2183–2192.

Friedel, R. H., T. E. Cayton, and A. Varotsou (2008), Detailed Observations of the outer radiation belt with LANL GPS instruments, *Eos Trans. AGU*, *88*(52), Abstract U13A-0042.

Golden, D. I., M. Spasojevic, and U. S. Inan (2009), Diurnal dependence of ELF/VLF hiss and its relation to chorus at L = 2.4, *J. Geophys. Res.*, *114*, A05212, doi:10.1029/2008JA013946.

Golden, D. I., M. Spasojevic, F. R. Foust, N. G. Lehtinen, N. P. Meredith, and U. S. Inan (2010), Role of the plasmapause in dictating the ground accessibility of ELF / VLF chorus, *J. Geophys. Res.*, *115*, A11211, doi:10.1029/2010JA015955.

Golden, D. I., M. Spasojevic, and U. S. Inan (2011), Determination of solar cycle variations of midlatitude ELF / VLF chorus and hiss via automated signal detection, *J. Geophys. Res.*, *116*, A03225, doi:10.1029/2010JA016193.

Hogg, R. V., and E. A. Tanis (1989), *Probability and Statistical Inference*, 3rd ed., Macmillan, New York.

Inan, U. S., and T. F. Bell (1977), The plasmapause as a VLF wave guide, *J. Geophys. Res.*, *82*(19), 2819–2827.

Jirícek, F., D. R. Shklyar, and P. Triska (2001), LHR effects in nonducted whistler propagation: New observations and numerical modeling, *Ann. Geophys.*, *19*, 147–157.

Kennel, C. F., and H. E. Petschek (1966), Limit on stably trapped particle fluxes, *J. Geophys. Res.*, *71*(1), 1–28.

Kimura, I. (1985), Whistler mode propagation in the earth and planetary magnetospheres and ray tracing techniques, *Space Spi. Rev.*, *42*, 449–466.

Lichtenberger, J. (2009), A new whistler inversion method, *J. Geophys. Res.*, *114*, A07222, doi:10.1029/2008JA013799.

Lichtenberger, J., C. Ferencz, R. L. Bodnár, D. Hamar, and P. Steinbach (2008), Automatic whistler detector and analyzer system: Automatic whistler detector, *J. Geophys. Res.*, *113*, A12201, doi:10.1029/2008JA013467.

Lichtenberger, J., C. Ferencz, D. Hamar, P. Steinbach, C. J. Rodger, M. A. Clilverd, and A. B. Collier (2010), Automatic Whistler Detector and Analyzer system: Implementation of the analyzer algorithm, *J. Geophys. Res.*, *115*, A12214, doi:10.1029/2010JA015931.

Manninen, J. (2005), Some aspects of ELF-VLF emissions in geophysical research, PhD thesis, University of Oulu, Oulu, Finland

Meredith, N. P., R. B. Horne, R. M. Thorne, and R. R. Anderson (2003), Favored regions for chorus-driven electron acceleration to relativistic

energies in the earth's outer radiation belt., *Geophys. Res. Lett.*, *30*(16), 1871, doi:10.1029/2003GL017698.
Moldwin, M. B., L. Downward, H. K. Rassoul, R. Amin, and R. R. Anderson (2002), A new model of the location of the plasmapause: CRRES results, *J. Geophys. Res.*, *107*(A11), 1339, doi:10:1029/2001JA009211.
Parrot, M., et al. (2004), Characteristics of magnetospherically reflected chorus waves observed by CLUSTER, *Ann. Geophys.*, *22*(7), 2597–2606.
Rosenberg, T. J., R. A. Helliwell, and J. P. Katsufrakis (1971), Electron precipitation associated with discrete very low frequency emissions, *J. Geophys. Res.*, *76*(34), 8445–8452.
Rosenberg, T. J., J. C. Siren, D. L. Matthews, K. Marthinsen, J. A. Holtet, A. Egeland, D. L. Carpenter, and R. A. Helliwell (1981), Conjugacy of electron mcrobursts and VLF chorus, *J. Geophys. Res.*, *86*(A7), 5819–5832.
Santolik, O., D. A. Gurnett, J. S. Pickett, and J. Chum (2009), Oblique propagation of whistler mode waves in the chorus source region, *J. Geophys. Res.*, *114*, A00F03, doi:10.1029/2009JA014586.
Sazhin, S. S., and M. Hayakawa (1992), Magnetospheric chorus emissions: A review, *Planet. Space Sci.*, *40*(5), 681–697.
Sazhin, S. S., K. Bullough, and M. Hayakawa (1993), Auroral hiss: A review, *Planet. Space Sci.*, *41*(2), 153–166.
Sheeley, B. W., M. B. Moldwin, H. K. Rassoul, and R. R. Anderson (2001), An empirical plasmasphere and trough density model: CRRES observations, *J. Geophys. Res.*, *106*(A11), 25,631–25,641.
Shimakura, S., M. Okada, M. Hayakawa, and Y. Tanaka (1986), The relationship between the polarization of whistlers and their dispersion, *J. Geophys. Res.*, *59*, 140–141.
Smith, A. J. (1994), VELOX: A new VLF/ELF receiver in Antarctica for the global geospace science mission, *J. Atmos. Sol. Terr. Phys.*, *57*(5), 507–524.
Smith, A. J., M. P. Freeman, and G. D. Reeves (1996), Postmidnight VLF chorus events, a substorm signature observed at the ground near L = 4, *J. Geophys. Res.*, *101*, 24,641–24,653.
Spasojevíc, M., and U. S. Inan (2005), Ground based VLF observations near L = 2.5 during the Halloween 2003 storm, *Geophys. Res. Lett.*, *32*, L21103, doi:10.1029/2005GL024377.
Summers, D., R. M. Thorne, and F. Xiao (1998), Relativistic theory of wave-particle resonant diffusion with application to electron acceleration in the magnetosphere, *J. Geophys. Res.*, *103*, 20,487–20,500.
Tsurutani, B. T., and G. S. Lakhina (1997), Some basic concepts of wave-particle interaction in collisionless plasmas, *Rev. Geophys.*, *35*(4), 491–502.
Wang, C., Q. Zong, F. Xiao, Z. Su, Y. Wang, and C. Yue (2011), The relations between magnetospheric chorus and hiss inside and outside the plasmasphere boundary layer: Cluster observation, *J. Geophys. Res.*, *116*, A07221, doi:10.1029/2010JA016240.